scientific reports

Check for updates

OPEN

Muon spectroscopy of a 12-phosphatetraphene with extremely efficient radical trapping properties

Shigekazu Ito[1]✉, Kohei Yasuda[1], Keisuke Ishihara[1], Victoria L. Karner[2], Kenji M. Kojima[2] & Iain McKenzie[2]

This paper describes muon spin spectroscopy studies of 12-phosphatetraphene stabilized by a peri-trifluoromethyl group and a meso-aryl substituent. Even though the prepared solution in tetrahydrofuran (THF) was quite dilute (0.060 M) for transverse-field muon spin rotation (TF-μSR) measurements, the π-extended heavier congener of tetraphene presented a pair of signals due to a muoniated radical from which the muon hyperfine coupling constant (hfc) was determined. This muoniated radical was produced by the diffusion-controlled regioselective addition of muonium (Mu = [μ^+e^-]) to the sp^2-hybridized phosphorus atom. The assignment of the muoniated radical structure was confirmed by observing a resonance due to the $I = 1/2$ (^{31}P) nucleus in a muon (avoided) level-crossing resonance (μLCR) spectrum. The ^{31}P hfc was determined from the resonance position, and a comparison with the value obtained from density functional theory (DFT) calculations indicated that the radical retained a flat π-delocalized tetracyclic skeleton. This higher energy structure is hypothesized to be preferable because of the increased zero-point energy of the light mass of the muon. The findings of this study could be fruitful in developing novel spin-functional materials featuring efficient radical capture and π-delocalized paramagnetic molecular systems.

Keywords Muon, Radicals, Heterocycles, Isotope effects, Reaction kinetics, DFT calculations

The exchange of skeletal sp^2 carbon atoms in polyaromatic hydrocarbons (PAHs) with heavier p-block elements reduces the HOMO-LUMO gap, which has attracted the interest of many researchers in chemistry, physics, and materials science. For example, group 14/15 elements have been used in the synthesis of congeners of naphthalene, anthracene, phenanthrene, and [7]helicene[1–12]. Although most heavier congeners of PAHs are unstable, designing appropriate peripheral substituents enables isolation under ordinary conditions and characterization of the physical properties of the π-electron systems. We used fluoroalkyl groups at the peri positions to stabilize 9-phosphaanthracene[3,13,14], which enabled chromatographic purification and characterization of physical properties including fluorescence and crystalline polymorphs[15]. Notably, the synthetic procedures of peri-trifluoromethylated 9-phosphaanthracenes can be applied for extensions of the π-electron system of 9-phosphaanthracene[16] and the synthesis of thienoacenes including fused phosphinine (a phosphorus analog of pyridine)[17].

Considering the importance of the radical reactions of anthracene from the perspectives of bioactivity, combustion science, and environmental science[18–21], we previously analyzed the radical reaction of a peri-trifluoromethylated 9-phosphaanthracene via muon spin rotation, relaxation, and resonance (μSR) spectroscopy[22]. A positive muon (μ^+) is an elementary particle classified as a lepton. High-intensity, spin-polarized beams of muons are available at several accelerator facilities around the world. In most insulating materials, a positive muon can capture an electron during the radiolysis process and form a muonium (Mu = [μ^+e^-]), which behaves chemically like a light isotope of hydrogen. The light H-atom surrogate Mu can add to the unsaturated parts in the organic molecule and produce a muoniated paramagnetic species. The muon hyperfine coupling constants (hfcs) of the muoniated radicals produced by the addition of Mu to organic compounds are considerably smaller than those of Mu itself (4463.3 MHz) because the unpaired electron is delocalized

[1]Department of Chemical Science and Engineering, School of Materials and Chemical Technology, Tokyo Institute of Technology, 2-12-1-H-113 Ookayama, Meguro-ku, Tokyo 152-8552, Japan. [2]Centre for Molecular and Materials Science, TRIUMF, 4004 Wesbrook Mall, Vancouver, BC V6T 2A3, Canada. [3]Dedicated to Prof. Hansjörg Grützmacher on the occasion of his 65th birthday. ✉email: ito.s.ao@m.titech.ac.jp

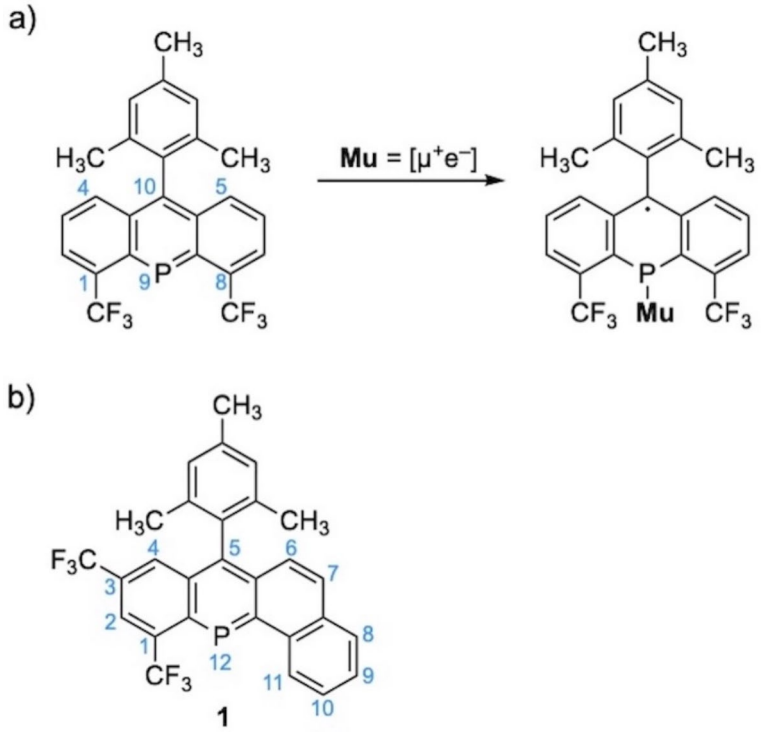

Fig. 1. (**a**) Reaction of a peri-trifluoromethylated 9-phosphaanthracene with muonium (Mu). (**b**) Chemical formula of 12-phosphatetraphene **1** for this μSR study.

over multiple atoms[23–26]. The muon hfc and the hfcs of other nuclei in the radical with nuclear spin $I > 0$ can be used to map the distribution of the unpaired electron and determine the structure of the radical. To date, muoniated radicals have been produced not only by the reaction of Mu with ordinary organic compounds such as benzenes, alkenes, alkynes, and aldehydes/ketones[27–29] but also by reactions with heavier congeners including imines, carbenes, and cyclobutane-1,3-diyls[30–32].

In our previous μSR study of a peri-trifluoromethylated 9-phosphaanthracene[22], we observed the regioselective addition of Mu to sp^2-type phosphorus, affording the single paramagnetic species, which was in sharp contrast with anthracene[33] and the acyclic phosphaalkenes producing the mixtures of the muonium (Fig. 1a)[34–36]. Notably, the hfc parameters of the muoniated 9-phosphaanthracene indicated a planar tricyclic system because the increased zero-point energy due to the muon of 1/9th mass of the proton cancels the trifluoromethyl effect. These findings suggest that μSR could clarify the unveiled characteristics of organic molecules as well as muon(ium) via chemical processes including H-surrogates and heavier PAHs.

We recently synthesized several π-extended derivatives of 9-phosphaanthracene. Figure 1b is a formula of 12-phosphatetraphene **1** as a π-extended phosphaanthracene[16]. The highly π-conjugated tetracyclic system in **1** would be promising for producing uniquely delocalized paramagnetic structures by capturing radicals; thus, **1** should be attractive for producing transient paramagnetic molecules via the muon isotope effect leading to the planar π-delocalized molecular skeleton. In this study, observation of muoniated **1** via μSR experiments was attempted, and the muonium radical was structurally characterized via DFT calculations. The amount of the sample seemed to be insufficient for μSR, but as a result, the use of a dilute solution sample **1** was advantageous for characterizing the considerable reactivity with muonium. The temperature dependence of the muoniated radical containing the *planar* 12-phosphatetraphene skeleton and the reaction dynamics of the addition of muonium were also investigated.

Materials and methods

A total of 120 mg of **1** was prepared according to the synthetic procedures in the literature[16]. A solution sample of 0.060 M (1 M = 1 mol dm^{-3}) **1** was prepared by using 4.0 mL degassed tetrahydrofuran (THF) in a glovebox. The THF solution was packed in the cell shown in Fig. 2.

The μSR measurements were performed at TRIUMF on the M15 beamline with the Helios spectrometer. The μSR techniques and their applications in chemistry have been extensively reviewed[23,24,27–32].

Density functional theory (DFT) calculations were performed via the Gaussian09 software package[37]. Hydrogen was used instead of muonium in the structure optimization. The normally optimized structure did not consider the isotope effect of muon increasing the zero-point energy and was revised to include the muonium radical of 9-phosphaanthracene[22]. The flat tetracyclic skeleton was maintained during the calculation. Conventional structural modifications involving increasing the bond length and angles around the muonium

Fig. 2. A solution sample of **1** in degassed THF (0.060 M) sealed in a μSR sample cell.

were attempted as the empirical vibrational averaging but were unsuccessful in simulating the experimental results.

Results and discussion

μSR of a peri-trifluoromethylated 12-phosphatetraphene

TF-μSR measurements were performed on a 0.060 M THF solution of **1**. It was expected that a 0.060 M solution sample of **1** would be too dilute to observe any muoniated radical by μSR. However, to our surprise and delight, a pair of signals due to a single type of muoniated radical was observed, as shown in Fig. 3a. The signals were confirmed to be real, as they shifted appropriately between measurements made in two different applied magnetic fields. The peak at + 36 MHz reflects the real peak at around − 36 MHz (ν_{12}), consistent with Figure S4 of ν_{μ} = 196 MHz in a 1.44 T transverse field. The amplitude of the ν_{12} signal increased dramatically with increasing temperature (Fig. 3b).

To observe a muoniated radical with TF-μSR, there must be efficient transfer of spin polarization from Mu to the muoniated radical. In the high magnetic field, this is approximately

$$P = \frac{\lambda^2}{\lambda^2 + \delta\omega^2} \tag{1}$$

where λ is the addition rate of Mu and equals k_{Mu}[**1**], where k_{Mu} is the second order Mu addition rate constant, [**1**] is the concentration of **1**, and $\delta\omega = \omega_{Mu} - \omega_R$ is the difference in precession frequencies in Mu and the radical. The physical interpretation is that the muon spins in Mu dephase prior to the reaction; if the rate is too slow or the field is too high, then muon polarization is lost. In the case of 9-phosphaanthracene, the muoniated radical was observed when a 0.16 M solution was used[22], and the more dilute conditions were inappropriate for observing the paramagnetic signals. In most relevant μSR studies of the phosphorus congeners of alkenes, 0.5 M solutions were used for observing the muonium adducts[34–36]. To observe a muoniated radical with a concentration of 0.06 M, the rate constant of addition has to be ~ 10^{10} M^{-1} s^{-1}, which is approaching the diffusion-controlled limit (10^{10}~10^{11} M^{-1} s^{-1})[24,38]. The increase in the amplitude of the radical signal is consistent with an increase in the diffusion coefficients of Mu and **1** due to the increasing temperature and decreasing viscosity of the THF solvent (Fig. 3b inset). As far as the authors know, comparable diffusion parameters on the regioselective muoniation at the P = C-containing molecule have never been reported.

In high magnetic fields, only the 1↔2 and 3↔4 transitions can be observed:

$$\upsilon_{12} = \nu_D - \frac{1}{2}A_\mu \tag{2}$$

$$\upsilon_{43} = \nu_D + \frac{1}{2}A_\mu \tag{3}$$

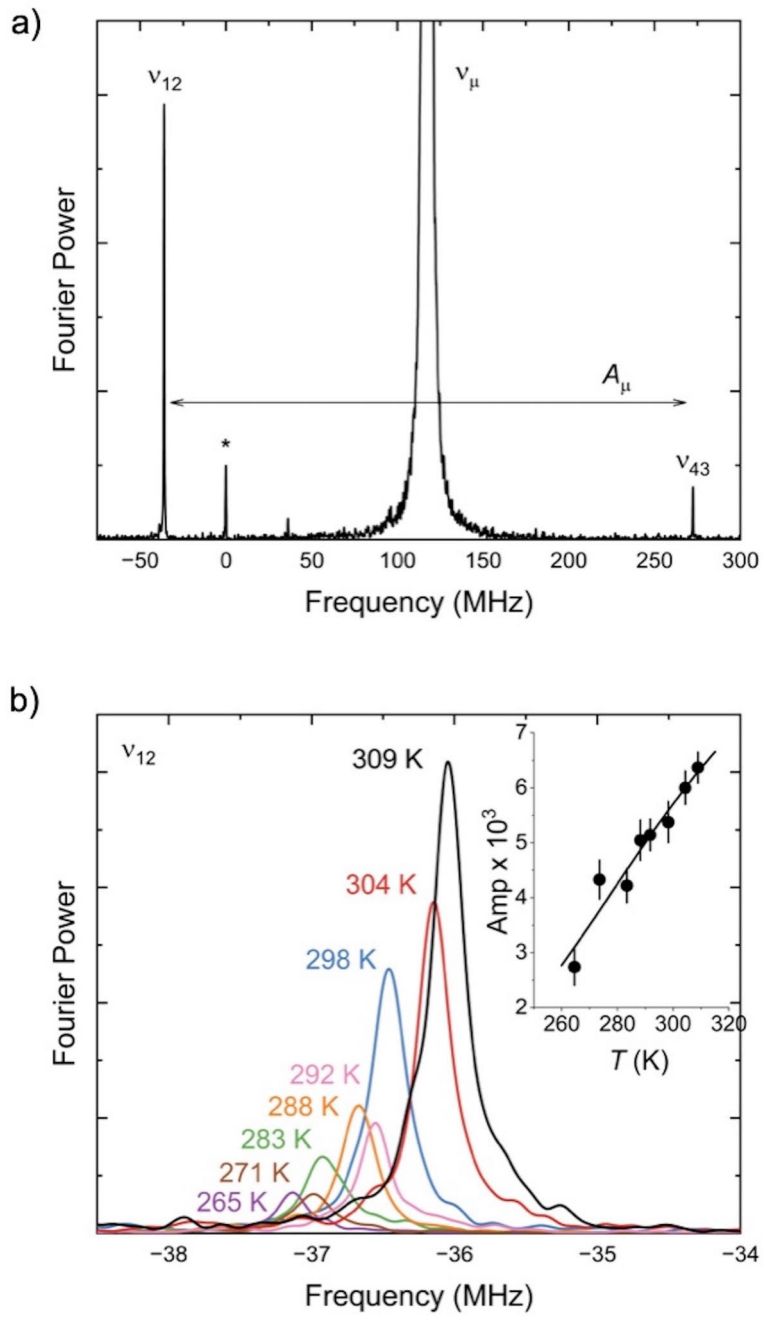

Fig. 3. (**a**) A Fourier transformed TF-μSR spectrum of a 0.060 M THF solution of **1** that was exposed to a beam of μ^+ at 309 K in a 0.86 T transverse magnetic field. A strong diamagnetic resonance of muon (ν_{μ}) appears at 117 MHz, and one pair of paramagnetic signals ν_{12} and ν_{43} means $A_{\mu} = 306.472 \pm 0.010$ MHz. The paramagnetic signal ν_{43} is small because of the time resolution of the spectrometer. The peak at 0 MHz marked with * is an artefact due to the Fourier transform. (**b**) The ν_{12} signal in the Fourier transformed TF-μSR spectra of a 0.060 M THF solution of **1** in a 0.86 T transverse magnetic field as a function of temperature. The inset graph shows the temperature dependence of the amplitude of the ν_{12} signal determined from fits in the time domain.

where ν_D is the precession frequency of muons in diamagnetic environments (closed shell: 135.53 MHz/T), and A_{μ} is the muon hfc. A_{μ} can be readily determined from the difference of the two radical precession signals, or if the higher frequency cannot be observed owing to the time resolution of the spectrometer, A_{μ} can be determined from ν_{12} and ν_D. A_{μ} is 306.969 ± 0.014 MHz at 298 K.

The hfcs of other nuclei can be measured via muon *avoided* level-crossing resonance (μLCR, alternatively referred to as avoided level-crossing muon spin resonance or ALC-μSR). In μLCR measurements, both the muon's spin and the magnetic field are oriented parallel to the muon's momentum. The muon's polarization is proportional to the asymmetry, which is the difference in the time-integrated number of positrons measured in the forward and backward directions divided by the total. Under most applied fields, the muon's spin does not evolve with time. However, there are certain magnetic fields where the spin states of the radical are nearly degenerate, which causes a mixing of the spin states. If the mixed states involve different muon spin orientations, there is a partial loss of spin polarization at the resonance field. In solution, resonances are only observed between spin states where M, which is the sum of the spin quantum numbers of the muon (μ), electron (e), and nucleus (k), does not change. These are called $\Delta M = 0$ or Δ_0 resonances. The resonance occurs at a magnetic field according to Eq. (4):

$$B_{\mathrm{LCR}}^{\Delta_0} = \frac{1}{2}\left[\frac{A_\mu - A_k}{\gamma_\mu - \gamma_k} - \frac{A_\mu + A_k}{\gamma_e}\right] \tag{4}$$

where γ_μ, γ_k, and γ_e refer to the gyromagnetic ratios of the muon, the nucleus k, and the electron, respectively. A_k is the hyperfine coupling constant of nucleus k.

The μLCR spectra of the 0.060 M THF solution of **1** are shown in Fig. 4a. There is a Δ_0 resonance at 750.6 ± 0.2 mT at 298 K. We know that this Lorentz-like resonance is not due to protons as the resulting proton hfc would be too large (~ 166 MHz). The addition of Mu at the secondary unsaturated carbons (positions 6 and 7 of **1**) would generate relatively preferable benzyl-type radicals[16]. These radicals have a CHMu methylene group, and with a muon hfc of ~ 307 MHz the value of the proton hfc should be ~ 80 MHz (see Fig. 5d and the Supporting Information). Radicals of this type would have Δ_0 resonances above 1 T. On the basis of the magnetic field and

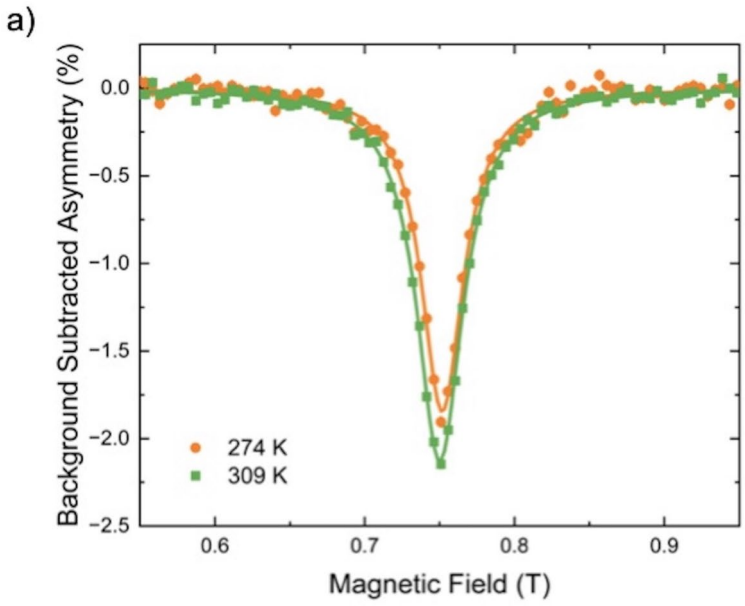

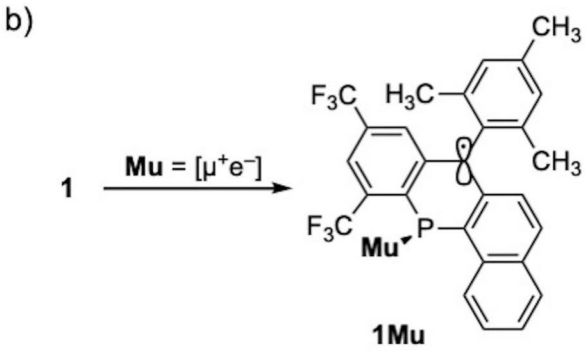

Fig. 4. (**a**) μLCR spectra of a 0.060 M solution of **1** in THF. The error bars are smaller than the data points. (**b**) Regioselective addition of muonium to the sp^2-type phosphorus in **1**, generating paramagnetic **1Mu**.

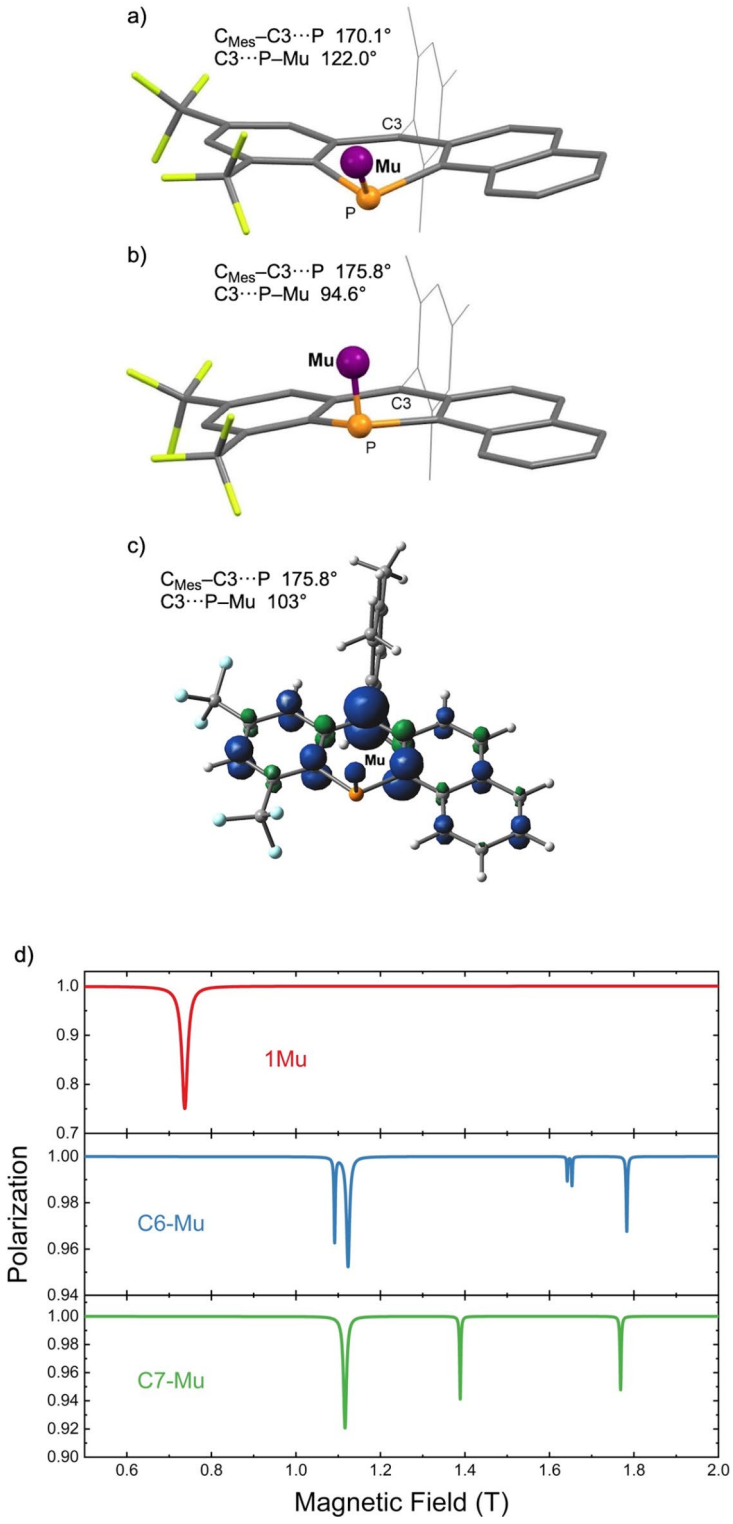

Fig. 5. (**a**) A normally optimized structure of **1Mu**. Hydrogen was used instead of Mu at the UB3LYP/def2-SVP level. (**b**) The alternative structure of **1Mu** maintains a flat tetracyclic system with an increased total energy of 1.59 kcal/mol. Modifying the C3···P–Mu(H) angle to 103° with increasing total energy (0.86 kcal/mol) provides the almost identical muon and ^{31}P hfc constants of 304.5 and 128.3 MHz, respectively, to the experimentally determined A_{μ} (307 MHz) and $A_{^{31}\mathrm{P}}$ (128 MHz) values. (**c**) The spin density (iso = 0.006, blue: α spin, green: β spin) of the modified structure from (**b**) indicates the delocalization of the unpaired electron over the planar tetracyclic skeleton. (**d**) Simulated μLCR spectra for the DFT-calculated structures of **1Mu** (**c**), **C6-Mu**, and **C7-Mu** (see Fig. 6).

the amplitude of the resonance, we have concluded that this resonance is due to ^{31}P. The ^{31}P hfc ($A_{^{31}\mathrm{P}}$) was determined via Eq. 4 and is 127.54 ± 0.04 MHz at 298 K. Based on the muon and ^{31}P hfcs, we have concluded that Mu regioselectively adds to the sp^2-hybridized phosphorus in **1** leading to **1Mu** (Fig. 4b). The relatively broad LCR signal (FWHM ~ 50 mT) might be due to the rotating CF_3 units containing ^{19}F nuclei of $I = 1/2$[39].

Other plausible positions of muoniation in **1**, which are C2, C4, C8-11, and the 2,4,6-$(CH_3)_3C_6H_2$ aromatic ring, would provide the corresponding cyclohexadienyl radical upon muoniation and would display muon hfcs of 450 ~ 500 MHz. Therefore, muoniation at the aromatic rings in **1** is excluded.

DFT calculations

The hyperfine parameters of **1Mu** were obtained from DFT calculations and compared with experimentally measured A_μ and $A_{^{31}\mathrm{P}}$ parameters to draw some conclusions about the radical's structure. The structure of **1Mu** was first optimized at the UB3LYP/def2-SVP level. Hydrogen was used instead of Mu for the geometry optimization and the minimum energy structure is shown in Fig. 5a. The initial coplanar tetracyclic system is distorted to a saddle-type shape because of the CF_3 group at the peri-position, and the C_{Mes}–C3···P (Mes = mesityl, 2,4,6-trimethylphenyl) and C3···P–Mu angles are 170.1 and 122.0°, respectively. The muon and ^{31}P hfcs of the normally optimized structure of **1Mu** are 211.4 and 148.2 MHz, respectively, and the calculated A_μ is significantly smaller than the experimentally determined value of 306.5 MHz. The DFT optimization using the H atom in place of Mu did not consider the light mass of the muon increasing zero-point energy, and accordingly, the structure in Fig. 5a should be corrected. In the muoniated cyclohexadienyl radical, the reduced muon hfc [$A_\mu' = A_\mu \cdot (\mu_p/\mu_\mu) = A_\mu/3.1833$, μ_p and μ_μ are magnetic moments of proton and muon, respectively] is 28% larger than the corresponding methylene A_p due to the approximately 4.9% longer C–Mu bond than C–H[23,24,27–29]. Such structural deviation into the energetically higher form is from the increased zero-point energy caused by the light mass of muon. Conventional structural modifications for the effects of muon were attempted by elongating the P–Mu(H) bond and scanning the angles around the phosphorus. However, these conventional methods were unsuccessful in simulating the experimental results (*vide infra*). Therefore, as we have previously done in the study of peri-trifluoromethylated 9-phosphaanthracene[22], the structure of the muoniated radical **1Mu** produced from the CF_3-substituted phosphatetraphene (**1**) was optimized with the constraint that the tetracyclic molecular skeleton should be flat. This resulted in an alternative structure shown in Fig. 5b. The C_{Mes}–C3···P and C3···P–Mu angles are 175.8 and 94.6°, respectively, and the calculated muon hfc of 294.8 MHz is close to the experimental data. On the other hand, the simulated hfc value of ^{31}P substantially deviated from the result of the μLCR. After some attempts, we found that changing the C3···P–Mu angle from 94.6° to 103° while increasing the total energy to 0.86 kcal/mol could simulate the comparable calculated muon and ^{31}P hfc parameters of 304.5 and 128.3 MHz, respectively. The additional structural modifications for Fig. 5b via 4% elongation of P–Mu provided the larger muon hfcs such as 329 MHz (C3···P–Mu 94.6°) and 341 MHz (C3···P–Mu 103°) and were overestimated. Figure 5c displays a plot of the spin density distribution over the modified flat form obtained by altering the C3···P–Mu angle and indicates considerable delocalization over the tetracyclic skeleton. The delocalized spin density over the flat molecular framework would enhance the overlap with the P–Mu bond, corresponding to the increased muon hfc and the proportionally increased ^{31}P hfc. Figure 5d displays a simulated μLCR spectrum for **1Mu** of Fig. 5c using the program Quantum[40,41] and is comparable with Fig. 4a showing the single, broad resonance around 750 mT. On the other hand, according to the Quantum calculations, the muoniation products at the C6 and C7 positions (**C6-Mu** and **C7-Mu**, Fig. 6) which would be possible to be produced (*vide infra*) should show several significant resonances at 1 ~ 1.8 T. Therefore, only **1Mu** is compatible with the experimental μLCR spectra in Fig. 4a. Table 1 summarizes the experimental and DFT-estimated hyperfine constants and the energetic parameters for **1Mu**. The normally optimized structure shown in Fig. 5a is incompatible with the experimental results even when the bond distance and angle around Mu(H) are modified (see Figure S6). Frequency analyses using the 0.1134 amu for muonium characterized the larger zero-point energies (ZPEs). On the other hand, the ΔE_{ZPE}(Mu-H) values comparing ZPE for each structure (**1Mu**_normal, **1Mu**_flat, **1Mu**_flat-modified) are proportional to the ΔE_{total} data, which is consistent with the structural deviation by the muon isotope effect. The increased zero-point energy (ZPE) was estimated for each calculated structure using 0.1134 amu for muonium. Table S1 shows the parameters of **C6-Mu** and **C7-Mu**, which are not comparable with the experimental data discussed above. The increase of ZPE for C–Mu is larger compared with P–Mu.

Figure 6 shows the distinguished coordinate reaction paths for Mu addition at different sites of **1** that produce **1Mu**, **C6-Mu**, and **C7-Mu**. Muoniation affording **1Mu** would proceed without activation energy, probably correlating with the instability of the P = C units. As indicated by the X-ray data, the C6 and C7 positions are relatively tolerant to muoniation because the 6-membered ring containing C6 and C7 lacks aromaticity as indicated by the small absolute value of Nucleus-Independent Chemical shift (NICS)[42,43] at the ring center [NICS(0) = −3.83][16]. Muoniation leading to **C6-Mu** would require an obvious activation energy (E_a = 1.7 kcal/mol) and would be affected by steric effect. In the case of **C7-Mu**, a quite small (or negligible) activation energy of 0.006 kcal/mol was observed probably due to steric effect[44]. It is surprising that this radical was not observed. For reference, both **C6-Mu** and **C7-Mu** are thermodynamically unstable compared with **1Mu**, which is correlated with the difference of stability between the P = C and C = C bonds. Both the experimental and theoretical μLCR spectra (Figs. 4a and 5d) are consistent with **1Mu**.

Temperature effect and thermodynamic parameters of the muoniated 12-phosphatetraphene

Figure 7a and b show the temperature dependences of A_μ and $A_{^{31}\mathrm{P}}$ determined by TF-μSR and μLCR, respectively. Both hfcs values decrease as the temperature increases, indicating that a higher temperature promotes a more stable form by reducing the C3···P–Mu angle in the flat form (see the Supporting Information).

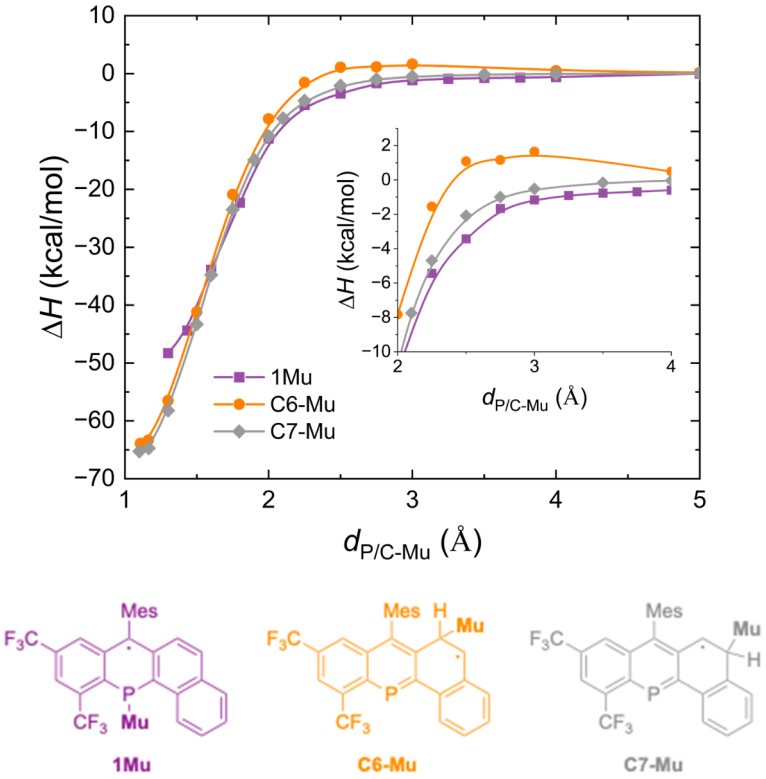

Fig. 6. Distinguished coordinate reaction paths (Δ*H*, kcal/mol) for Mu addition to the sp^2-phosphorus atom in **1** yielding **1Mu** and Mu addition to the 6- and 7-positions in **1** yielding **C6-Mu** and **C7-Mu**. The inset shows an enlarged plot indicating the quite small barrier leading to **C7-Mu**. The structures of the resulting radicals are shown below.

Parameter	Experimental	1Mu_normal[c] [Fig. 5a]	1Mu_flat[c] [Fig. 5b]	1Mu_flat-modified[d] [Fig. 5c]
Muon hfc/MHz	307.0[a]	211.4 (237.4)[e] (223.7)[f]	294.8 (328.6)[e]	304.5 (341.3)[e]
^{31}P hfc/MHz	127.5	148.2 (156.3)[e] (81.3)[f]	80.5 (87.0)[e]	128.3 (137.7)[e]
ΔE_{total}/kcal mol^{-1}	–	0.00 (+0.69)[e] (+4.08)[f]	+1.59 (+2.24)[e]	+2.44 (+3.17)[e]
ΔE_{ZPE}(Mu-H)[g]/kcal mol^{-1}	–	11.03	10.56	10.44

Table 1. Experimental and DFT-estimated hyperfine parameters of **1Mu**. [a]TF-μSR, THF solution, 309 K. [b]TF-μSR, THF solution, 309 K. [c]UB3LYP/def2-SVP. [d]UB3LYP/def2-SVP. The metric parameters except for the C3···P–Mu(H) angle of 103.0° are identical with **1Mu**_flat. [e]UB3LYP/def2-SVP. The P–Mu distance is 4% elongated from **1Mu**_flat. [f]UB3LYP/def2-SVP. Except for the C3···P–Mu(H) angle of 105.0°, the metric parameters are identical with **1Mu**_normal. [g]UB3LYP/def2-SVP. The zero-point energy difference between muonium of 0.1134 amu and hydrogen for each optimized or modified structure.

The temperature dependence of A_μ in **1Mu** is comparable to that in $MuCH_2$-C·$(CH_3)_2$[45–47], and the deviation of A_{31P} is proportional to that of A_μ. The small changes in hfcs would correlate with the considerable inversion barrier around phosphorus of ~30 kcal/mol. In contrast to the previous study on 9-phosphaanthracene[22], **1** is a prochiral molecule, and thus the muoniation product **1Mu** should be a mixture of chiral paramagnetic molecules[48]. When **1** could form distinguished chiral conformation, the muonium adducts should be diastereomeric and show two separate hfcs. In the case of **1**, the TF-μSR and μLCR did not separate, and thus **1** would not form chiral structures in irradiation of muon beam in tetrahydrofuran.

Conclusion

The reactions of a phosphorus congener of PAHs, peri-trifluoromethylated 12-phosphatetraphene **1**, with Mu, arguably the simplest free radical, were investigated via μSR spectroscopy. Mu added exclusively to the phosphorus. This highly regioselective muoniation was promoted by the highly reactive sp^2-hybridized phosphorus in **1**. Notably, the paramagnetic signals of the muonium adduct were observed even when the dilute solution of **1** (0.060 M in THF) was used, in contrast to the μSR studies of 9-phosphaanthracene and most organic compounds. The hyperfine parameters of muon (A_μ) and ^{31}P (A_{31P}) included the effect of the muon increasing zero-point energy, which promoted the

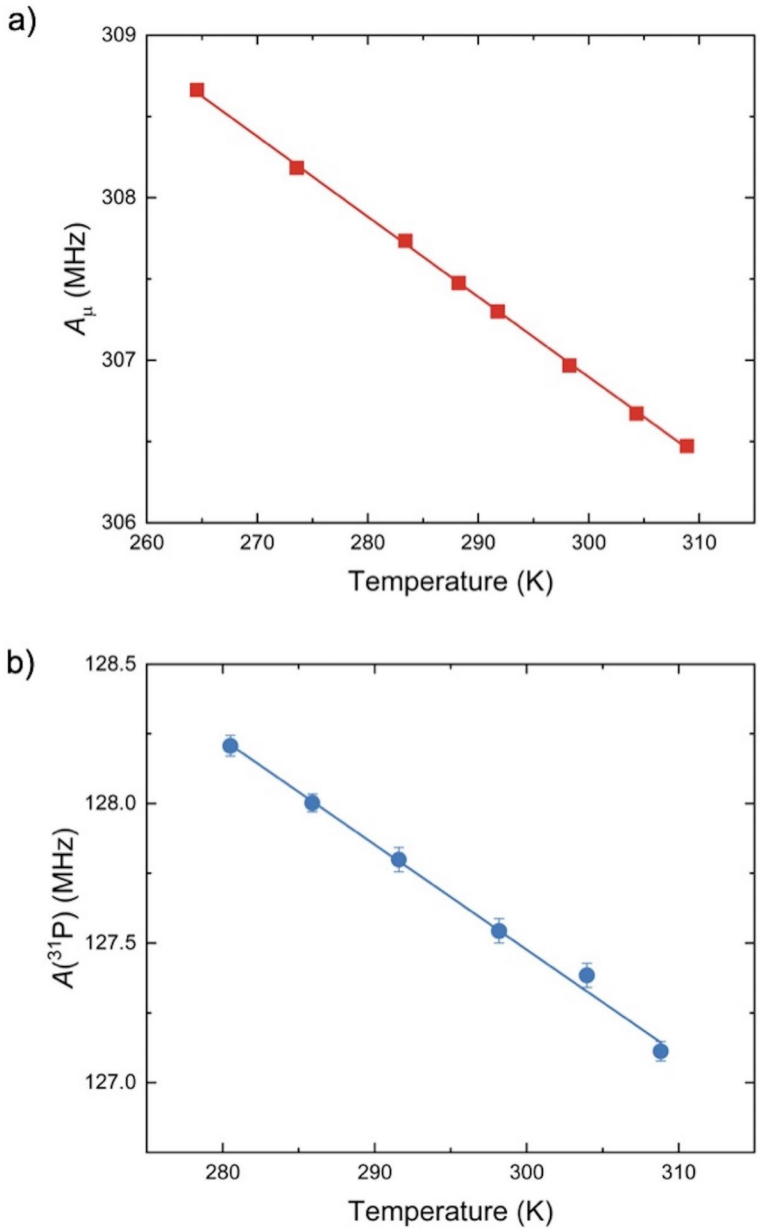

Fig. 7. (**a**) Temperature dependence of the muon hyperfine coupling constant of the Mu adduct of **1**. (**b**) Temperature dependence of the ^{31}P hyperfine coupling constant of the Mu adduct of **1**.

maintenance of the flat molecular framework of 12-phosphatetraphene and avoided the thermodynamically preferable saddle-type tetracyclic skeleton. The positive A_μ and A_{31P} parameters decreased with increasing temperature, which was comparable with the cases of $H_2C{=}C(CH_3)_2$[45–47] and biacetyl[48,49]. Additionally, the dynamics of muoniation to **1** were qualitatively discussed by using the relaxation parameters.

The results of this study strongly suggest that the π-extended phosphorus congener of a PAH, tetraphene, is useful for radical (spin) trapping on the basis of regioselective radical addition. Applications of **1** based on the basis of the findings from the μSR studies are now attempted. Additionally, other phosphorus congeners of PAHs such as phosphabenzotetraphenes and phosphatetracenes[16] would be attractive. Subsequent μSR studies on other phosphorus congeners of PAHs are in due course.

Data availability

All the data generated or analyzed during this study are included in this published article and supporting information. The μSR data are stored at TRIUMF.

Received: 15 August 2024; Accepted: 24 December 2024
Published online: 07 January 2025

References

1. de Graaf, H. G. & Bickelhaupt, F. 2-Phosphanaphthalenes. *Tetrahedron* **31**, 1097–1103 (1975).
2. Märkl, G., Kallmünzer, A., Nöth, H. & Pohlmann, K. Zur Umsetzung Von Diphenylketen Mit tert-butylphosphaethin Bildung eines 1-Phosphanaphthalins. *Tetrahedron Lett.* **33**, 1597–1600 (1992).
3. de Koe, P. & Bickelhaupt, F. Dibenzo[*b*,*e*]phosphorin. *Angew Chem. Int. Ed. Engl.* **6**, 567–568 (1967).
4. Teunissen, H. T. et al. Diels-Alder reactions of trichlorophosphaethene. *J. Org. Chem.* **60**, 7439–7444 (1995).
5. Beránek, T. et al. Synthesis of 2-phospha[7]helicene, a helicene with a terminal phosphinine ring. *Org. Lett.* **24**, 4756–4761 (2022).
6. Ashe, A. J., Fang, X. & Kampf, J. W. 1-Arsanaphthalene. The structure of tricarbonyl(2-trimethylsilyl-1-arsanaphthalene) molybdenum. *Organometallics* **20**, 2109–2113 (2001).
7. Jutzi, P. & Deuchert, K. 9-Arsaanthracene. *Angew Chem. Int. Ed. Engl.* **8**, 991–992 (1969).
8. Vermeer, H. & Bickelhaupt, F. Dibenz[b,e]arsenine (9-Arsaanthracene). *Angew Chem. Int. Ed. Engl.* **8**, 992 (1969).
9. Bickelhaupt, F., Lourens, R., Vermeer, H. & Weustink, R. J. M. Attempted syntheses of 9-stibaanthracene and 10-phenyl-9-stibaanthracene. *Recl. Trav Chim. Pays-Bas*. **98**, 3–4 (1979).
10. Takeda, N., Shinohara, A. & Tokitoh, N. The first stable 9-silaanthracene. *Organometallics* **21**, 256–258 (2002).
11. Tokitoh, N. New Progress in the Chemistry of stable metallaaromatic compounds of heavier Group 14 elements. *Acc. Chem. Res.* **37**, 86–94 (2004).
12. Tokitoh, N. Synthesis of aromatic species containing a heavier group 14 element by taking advantage of kinetic stabilization. *Bull. Chem. Soc. Jpn*. **77**, 429–441 (2004).
13. de Koe, P. & Bickelhaupt, F. 10-Phenyldibenzo[b,e]phosphorin. *Angew Chem. Int. Ed. Engl.* **7**, 889–890 (1968).
14. Jongsma, G., Vermeer, H., Bickelhaupt, F., Schäfer, W. & Schweig, A. 10-methyl-9-phosphaanthracene. *Tetrahedron* **31**, 2931–2935 (1975).
15. Ito, S., Koshino, K. & Mikami, K. CF_3-Inspired synthesis of air-tolerant 9-phosphaanthracenes that feature fluorescence and crystalline polymorphs. *Chem. Asian J.* **13**, 830–837 (2018).
16. Yasuda, K. & Ito, S. A π-extension process from 9-phosphaanthracene leading to phosphatetraphenes and phosphatetracenes. *ChemPlusChem* **88**, e202300277 (2023).
17. Matsuo, K. et al. Phosphaacene as a structural analog of thienoacenes for organic semiconductors. *Chem. Commun.* **58**, 13576–13579 (2022).
18. Farenhorst, E. & Kooyman, E. C. Relative reactivities of substituted anthracenes towards the addition of 2-cyano-2-propyl radicals. *Nature* **175**, 598–599 (1955).
19. Mahoney, L. R. Reactions of Peroxy radicals with Polynuclear Aromatic compounds. II. Anthracene in Chlorobenzene. *J. Am. Chem. Soc.* **87**, 1089–1096 (1965).
20. Ananthula, R., Yamada, T. & Taylor, P. H. Kinetics of OH radical reaction with anthracene and anthracene-d_{10}. *J. Phys. Chem. A* **110**, 3559–3566 (2006).
21. Jia, H. et al. Formation and stabilization of environmentally persistent free radicals induced by the interaction of anthracene with Fe(III)-modified clays. *Environ. Sci. Technol.* **50**, 6310–6319 (2016).
22. Koshino, K., Kojima, K. M., McKenzie, I. & Ito, S. Muonium addition to a peri-trifluoromethylated 9-phosphaanthracene producing a high-energy paramagnetic π-conjugated fused heterocycle. *Angew Chem. Int. Ed.* **60**, 24034–24038 (2022).
23. Blundell, S. J., de Renzi, R., Lancaster, T. & Pratt, F. L. (eds) *Eds. Muon spectroscopy – An Introduction* (Oxford University Press, 2022).
24. Fleming, D. G., McKenzie, I. & Percival, P. *W. Muon spin spectroscopy – Methods and Applications in Chemistry and Materials Science* (Wiley, 2024).
25. Mohr, P. J., Newell, D. V. & Taylor, B. N. CODATA recommended values of the fundamental physical constants: 2014. *Rev. Mod. Phys.* **88**, 035009 (2016).
26. Kanda, S. et al. New precise spectroscopy of the hyperfine structure in muonium with a high-intensity pulsed muon beam. *Phys. Rev. B*. **815**, 136154 (2021).
27. McKenzie, I. The positive muon and μSR spectroscopy: powerful tools for investigating the structure and dynamics of free radicals and spin probes in complex systems. *Annu. Rep. Prog Chem. Sect. C: Phys. Chem.* **109**, 65–112 (2013).
28. McKenzie, I. & Roduner, E. Using polarized muons as ultrasensitive spin labels in free radical chemistry. *Naturwissenschaften* **96**, 873–887 (2009).
29. Rhodes, C. J. Muonium—the second radioisotope of hydrogen—and its contribution to free radical chemistry. *J. Chem. Soc. Perkin Trans. 2* 1379–1396 (2002).
30. West, R., Samedov, K. & Percival, P. W. Silicon meets cyclotron: Muon spin resonance of organosilicon radicals. *Chem. Eur. J.* **20**, 9184–9190 (2014).
31. West, R. & Percival, P. W. Organosilicon compounds meet subatomic physics: Muon spin resonance. *Dalton Trans.* **39**, 9209–9216 (2010).
32. Ito, S. Muon spin rotation/resonance (μSR) for studying radical reactivity of unsaturated organophosphorus compounds. *Chem. Eur. J.* **28**, e202200843 (2022).
33. Macrae, R. M., Reid, I. D., von Schütz, J. U. & Nagamine, K. Order–disorder transition in anthracene/tetracyanobenzene probed by muonium-substituted radicals. *Phys. B.* **289–290**, 616–619 (2000).
34. Chandrasena, L. et al. Free radical reactivity of a phosphaalkene explored through studies of radical isotopologues. *Angew Chem. Int. Ed.* **58**, 297–301 (2019).
35. Walsgrove, H. T. G., Percival, P. W. & Gates, D. P. Probing radical addition to 1-phosphabutadienes by employing muonium as a light isotope of hydrogen. *Chem. Eur. J.* **30**, e202302869 (2024).
36. Samedov, K. et al. Free radical chemistry of phosphasilenes. *Angew Chem. Int. Ed.* **59**, 16007–16012 (2020).
37. Gaussian 09, Revision B.01, Frisch, M. J., Trucks, G. W., Schlegel, H. B., Scuseria, G. E., Robb, M. A., Cheeseman, J. R., Scalmani, G., Barone, V., Mennucci, B., Petersson, G. A., Nakatsuji, H., Caricato, M., Li, X., Hratchian, H. P., Izmaylov, A. F., J. Bloino, Zheng, G., Sonnenberg, J. L., Hada, M., Ehara, M., Toyota, K., Fukuda, R., Hasegawa, J., Ishida, M., Nakajima, T., Honda, Y., Kitao, O., Nakai, H., Vreven, T., Montgomery, Jr., J. A., Peralta, J. E., Ogliaro, F., Bearpark, M., Heyd, J. J., Brothers, E., Kudin, K. N., Staroverov, V. N., Keith, T., Kobayashi, R., Normand, J., Raghavachari, K., Rendell, A., Burant, J. C., Iyengar, S. S., Tomasi, J., Cossi, M., Rega, N., Millam, J. M., Klene, M., Knox, J. E., Cross, J. B., Bakken, V., Adamo, C., Jaramillo, J., Gomperts, R., Stratmann, R. E., Yazyev, O., Austin, A. J., Cammi, R., Pomelli, C., Ochterski, J. W., Martin, R. L., Morokuma, K., Zakrzewski, V. G., Voth, G. A., Salvador, P., Dannenberg, J. J., Dapprich, S., Daniels, A. D., Farkas, O., Foresman, J. B., Ortiz, J. V., Cioslowski, J. & Fox, D. J. Gaussian 09, Revision B.01, Gaussian Inc., Wallingford CT (2010).
38. Percival, P. W. Muonium Chemistry. *Radiochim. Acta* **26**, 1–14 (1979).
39. Fleming, D. G. et al. (eds) (Jun),. Hyperfine coupling constants of muonium-substituted cyclohexadienyl radicals in the gas phase: C_6H_6Mu, C_6D_6Mu, C_6F_6Mu. *Appl. Magn. Res.* **13**, 181–194 (1997).
40. McKenzie, I., Karner, V. L. & Scheuermann, R. Analysis of avoided level crossing muon spin resonance spectra of muoniated radicals in anisotropic environments: estimation of muon dipolar hyperfine parameters for lorentzian-like Δ_1 resonances. *Quantum Beam Sci.* **8**, 15 (2024).
41. Lord, J. S. Computer simulation of muon spin evolution. *Phys. B.* **374–375**, 472–474 (2006).
42. Schleyer, P. R., Maerker, C., Dransfeld, A., Jiao, H. & Hommes, N. J. R. v. E. Nucleus-independent chemical shifts: a simple and efficient aromatic probe. *J. Am. Chem. Soc.* **118**, 6317–6318 (1996).

43. Chen, Z., Wannere, C. S., Corminboeuf, C. & Puchta, R. Schleyer. P. v. R. Nucleus-independent chemical shifts (NICS) as an aromaticity criterion. *Chem. Rev.* **105**, 3842–3888 (2005).
44. DFT calculations. of tetraphene ($C_{18}H_{12}$) showed no activation energy for muoniation at the 7-position.
45. Roduner, E. et al. Muonium substituted organic free radicals in liquids. Muon-electron hyperfine coupling constants of alkyl and allyl radicals. *Chem. Phys.* **67**, 275–285 (1982).
46. Percival, P. W. et al. J. Intramolecular motion in the tert-butyl radical as studied by muon spin rotation and level-crossing spectroscopy. *Chem. Phys.* **127**, 137–147 (1988).
47. Roduner, E. et al. Quantum phenomena and solvent effects on addition of hydrogen isotopes to benzene and to dimethylbutadiene. *Ber Bunsenges Phys. Chem.* **94**, 1224–1230 (1990).
48. Roduner, E. & Reid, I. D. Hyperfine and structural isotope effects in muonated cyclohexadienyl and cyclopentyl radicals. *Isr. J. Chem.* **29**, 3–11 (1989).
49. Rhodes, C. J., Reid, I. D. & Macrae, R. M. The first observation of a muonium-carbonyl adduct with a negative muon coupling constant. *Chem. Commun.* 2157–2158 (1999).

Acknowledgements
This work was supported in part by JSPS KAKENHI Grant Numbers 19H02685, and 22K19023. Financial support was obtained from Nissan Chemical Corporation. Tian Zhang and Prof. Derek P. Gates of The University of British Columbia supported the preparation of the solution samples for μSR.

Author contributions
Kohei Yasuda and Keisuke Ishihara synthesized the sample for μSR. μSR measurements and the data analyses were performed by Shigekazu Ito, Victoria Karner, Kenji M. Kojima, and Iain McKenzie. DFT calculations were performed by Shigekazu Ito and Kohei Yasuda. All authors read and approved the final manuscript.

Funding
This work was supported in part by JSPS KAKENHI Grant Numbers 19H02685, and 22K19023.

Declarations

Competing interests
The authors declare no competing interests.

Additional information
Supplementary Information The online version contains supplementary material available at https://doi.org/10.1038/s41598-024-84611-w.

Correspondence and requests for materials should be addressed to S.I.